ORIGINAL PAPER

Artificial neural network for predicting the performance of waste polypropylene plastic-derived carbon nanotubes

H. U. Modekwe[1] · A. T. Akintola[1] · O. O. Ayeleru[2] · M. A. Mamo[3] · M. O. Daramola[4] · K. Moothi[5]

Abstract

In this study, an artificial neural network model using function fitting neural networks was developed to describe the yield and quality of multi-walled carbon nanotubes deposited over NiMo/CaTiO$_3$ catalyst using waste polypropylene plastics as cheap hydrocarbon feedstock using a single-stage chemical vapour deposition technique. The experimental dataset was developed using a user-specific design with four numeric factors (input variable): synthesis temperature, furnace heating rate, residence time, and carrier gas (nitrogen) flow rate to control the performance (yield and quality) of produced carbon nanotubes. Levenberg–Marquardt algorithm was utilized in training, validating, and testing the experimental dataset. The predicted model gave a considerable correlation coefficient (R) value close to 1. The presented model would be of remarkable benefit to successfully describe and predict the performance of polypropylene-derived carbon nanotubes and show how the predictive variables could affect the response variables (quality and yield) of carbon nanotubes.

Keywords Artificial Neural Network · Modelling · Plastic-derived carbon nanotubes · Quality · Waste polypropylene plastics · Yield

Introduction

Carbon nanotubes (CNTs) are synthesized by arc discharge, laser ablation, and chemical vapour deposition (CVD) techniques. Amongst the methods proposed for CNTs production, the CVD technique has been applauded over other techniques for large-scale CNTs synthesis. CVD allows for scale-up and precise control of CNTs orientation, alignment, diameter, length, purity, yield, etc. (Bazargan and Mckay 2012; Raji and Sobhan 2013). This method is simple and cheap with less energy consumption and minimal pollution compared to other techniques (Bazargan and Mckay 2012; Raji and Sobhan 2013). The unique thermal, electrical, mechanical, and high aspect ratio properties of CNTs (Bazargan and Mckay 2012) have been the driver for the growing demand (market) in applications such as polymer additives, catalysts, gas-discharge tubes in telecom networks, electron field emitters for cathode ray lighting elements, flat panel display, electromagnetic-wave absorption & shielding, hydrogen storage, energy conversion, lithium-battery anodes, nanotube composites (by coating or filling), nano-electrodes, nanolithography, cancer drug delivery, sensors, reinforcements in composites, and supercapacitor, CO$_2$ adsorption, wastewater treatment, etc. (Rao et al. 2018).

✉ H. U. Modekwe
uche_lyne2@yahoo.com; uchelyne2@gmail.com

[1] Renewable Energy and Biomass Research, Department of Chemical Engineering, University of Johannesburg, P. O. Box 17011, Johannesburg 2028, South Africa

[2] Centre for Nanoengineering and Advanced Materials, University of Johannesburg, P.O. Box 17011, Johannesburg 2028, South Africa

[3] Research Centre for Synthesis and Catalysis, Department of Chemical Science, Faculty of Science, Doornfontein Campus, University of Johannesburg, P. O. Box 17011, Johannesburg 2028, South Africa

[4] Department of Chemical Engineering, Faculty of Engineering, Built Environment and Information Technology, University of Pretoria, Private Bag X20 Hatfield, Pretoria 0028, South Africa

[5] Faculty of Engineering, School of Chemical and Minerals Engineering, North-West University, Potchefstroom 2520, South Africa

🖄 Springer

Increasing interest in CNTS in different applications by end-users and manufacturers is dependent on its quality (purity) and product cost of CNTs. Several methods including near-infrared optical spectroscopy, selected area electron microscopy (in transmission electron microscopy), thermogravimetry, Raman spectroscopy, X-ray diffraction, and fluorescence analysis have been proposed for assessing the quality and purity of carbon nanotubes (Das et al. 2015; Modekwe et al. 2021a). Raman spectra of CNTs provide general unique information about the structure and 1D properties of nanotubes. Other information such as nanotubes graphitic and imperfections as well as accurate measures of the phonon frequencies and electronic structures of nanomaterials could also be obtained using the Raman spectroscopic method (Dresselhaus et al. 2005; Lefrant et al. 2009; Lehman et al. 2011).

The high cost of CNTs resulting from the high cost of high-demand pure chemical feedstocks such as methane, acetylene, etc. could have a negative impact on the growth of the CNTs market. Therefore, the economies of utilizing waste plastics products as cheap carbon feedstock could be the cutting-edge measure to reduce the production cost as well as the unit price of CNTs (Modekwe et al. 2024). To date, the current production, and yield of CNTs derived from plastics are relatively low compared to the actual carbon content, in addition to the lack of defined structure and uniformity in plastic-derived CNTs. It is important that a relationship is proposed that relates the plastic type, catalyst composition, and CVD process conditions to the purity (quality) and yield of CNTs. Therefore, developing an efficient and appropriate predictive model that relates the yield and quality of CNTs obtained from waste PP to the production variables is very important.

Different modelling methods such as computational fluid dynamics (CFD), chemical kinetic modelling, response surface methodology (RSM), etc. have been applied in modelling the nucleation and growth of CNTs as well as predicting the yield and structure of CNTs (Raji and Sobhan 2013). RSM, for example, has gained recognition in various fields such as catalyst design and engineering, materials science, etc. as one of the modelling techniques (Yang et al. 2004; Sedighi et al. 2011). Kukovecz et al. (2005) utilized the statistical design of experiment to optimize and obtain the model that describes carbon yield and single walled carbon nanotubes (SWCNT) quality during catalytic chemical vapour deposition (CCVD) growth of CNTs over FeMo/MgO catalyst using acetylene as carbon precursor. According to their study by optimizing the interaction between process variables such as reaction temperature, reaction time, preheating time, catalyst mass,

C_2H_2 volumetric flow rate, and Argon volumetric flow rate, a trade-off between yield and quality of SWCNT using quality descriptor number (QDN) was achieved. Similarly, Bajad and Co-workers (Bajad et al. 2017) utilized statistical analysis to model and predict CNT yield within a range of input variables (recycle ratio, reaction time, pyrolysis temperature, and synthesis temperature) using $Ni_4Mo_{0.2}MgO$ catalyst and mixed plastic waste as carbon feedstock in a multi-core reactor.

Machine learning (ML) through artificial neural network (ANN), has gained interesting attention recently in chemical processes, such as in catalyst design, process modelling of complex chemical reactions, optimization of material properties, and process parameter control as another fitting data technique (Kusumo et al. 2019; Krasnikov et al. 2023). ANN are data-processing tools with machine learning potentials comprising interconnected nodes known as neurons (Deniz et al. 2017). These networks of neurons are trained to perform specific tasks by adjusting network parameters (Deniz et al. 2017). Very few studies have utilized the ANN method in predicting models for the nucleation and growth processes of CNTs. Lakovlev et al. (2019) applied ANN to process experimental datasets using growth temperature, residence time, and pressures of CO, CO_2, and ferrocene as input variables and at the same time predict the performance (yield, defectiveness, mean, and standard deviation of the diameter distribution) of SWCNTs grown by aerosol CVD synthesis method based on Boudouard Reaction. Aci and Avci (2016) also utilized four different ANN algorithms (feed-forward neural network, function fitting neural network, cascade-forward neural network, and generalized regression neural network) to predict models that could calculate atomic coordinates of CNTs fast and accurately. Similarly, Abad et al. (2017) synthesized bamboo-like structured MWCNTs from the predicted output value of the model trained from six growth parameters which were utilized as the input data using the multilayered perceptron neural network technique in evaluating the CNTs' diameter. The developed predictive model showed that the average CNTs diameter were of negligible error range of 7% when compared to the experimental result. Signifying that the trained ANN model was able to predict the precise CNTs' diameter.

This study aimed to develop an advanced and better predictive model using ANN which could predict yield and quality of CNTs grown from waste polypropylene plastics over NiMo/CaTiO$_3$ catalyst. A quantitative correlation between predictors, that is CVD growth parameters (synthesis temperature, residence time, heating rate, and inert (N_2) gas flow rate) and CNTs yield, and quality was

developed. Here, for the first time, a mathematical model was developed using machine learning (ANN) to describe the performance (yield and quality) of CNTs synthesized from waste PP over NiMo/CaTiO$_3$ catalyst. The predictive model using ML is a novel approach to describing the performance of waste plastic-derived CNTs through the processing of experimental datasets using various CVD parameters. Unlike other modelling approaches, ANN does not necessitate the formulation of intricate and multifaceted numerical equations. Again, ANN offers high prediction accuracy irrespective of the efficacy of the underlying process variables.

Materials and methods

Preparation of catalyst

Titanium (IV) isopropoxide (TTIP) (AR, 97% purity, Sigma-Aldrich), ammonium molybdate tetrahydrate (AR, 99% purity), nickel (II) nitrate hexahydrate (AR, 99% purity), and calcium carbonate (AR) were obtained from ACE (PTY) LTD.; additive-citric acid anhydrous, (AR, 99% purity) (purchased from Rochelle Chemicals and Laboratory equipment company) ethanol and deionized water were used in the synthesis. All reagents were used as received without additional purification. A conventional sol–gel method was employed for the preparation of NiMo/CaTiO$_3$ catalyst with a molar ratio of 4:1:2. The Ca/Ti content in the support was kept at 1:1. Detailed description of the experimental procedure for the preparation and characteristics of NiMo/

CaTiO$_3$ catalyst have previously been presented in an earlier publication (Modekwe et al. 2020).

Design of experiment

The experimental matrix was initiated using the Design Expert v11 built-in custom design model. Based on the literature and in order to reduce the cost of the experiment, four numeric factors namely: temperature (℃), heating rate (℃/min), time (min), and carrier gas flow rate (mL/min) were considered. The observed responses comprise the quality and yield of multi-walled carbon nanotubes produced from waste polypropylene plastic as hydrocarbon feedstock over NiMo/CaTiO$_3$ catalyst using a single-stage CVD technique. Nonetheless, other factors that could influence the yield and quality of CNTs are catalyst composition, reactor type, and catalyst preparation method. However, these variables are not considered in this study. The experimental matrix is presented in Table 1.

Synthesis of CNTs

CNTs were synthesized by the single-stage CVD method and waste PP plastics were sourced from used household food containers. The food containers were washed, sun-dried, and cut into small sizes using a Retsch SM 200 jaw crusher (Retsch GmbH, Germany). The procedure for the synthesis of CNTs from waste PP using single-stage catalytic CVD has been described in detail elsewhere (Modekwe et al. 2021b). All 13 runs were undertaken using Ni/Mo/CaTiO$_3$ catalyst with a similar molar ratio of 4:1:2.

Table 1 Experimental design of process variables

Numerical factors Experimental run	Factor 1 A: Synthesis temperature (°C)	Factor 2 B: Furnace heating rate (°C/min)	Factor 3 C: Residence time (min)	Factor 4 D: Carrier gas (N$_2$) flow rate (mL/min)
1	600	5	25	120
2	600	10	30	120
3	700	10	25	70
4	800	15	25	100
5	800	5	25	100
6	800	10	30	100
7	600	10	20	100
8	800	10	20	70
9	600	15	25	120
10	700	15	30	120
11	700	5	30	100
12	700	5	20	100
13	700	15	20	120

Purification of CNTs

Synthesized CNTs were ground to powder using agate mortar and pestle and the resultant powdery carbonaceous materials underwent two-step oxidative purification: (1) In air; air oxidation was carried out at 450 ℃, to remove amorphous carbonaceous materials, this temperature was based on DTG results from our previous study (Modekwe et al. 2020), when the set temperature was attained, the set-up was held for 40 min. Thereafter, the furnace was switched off and the sample was allowed to cool. (2) The air-oxidized sample was treated with about 200 ml of 0.1 M nitric acid sonicated for 10 min. All content was transferred into a round bottom flask and refluxed under vigorous stirring for 2 h at 100 ℃. The mixture was cooled and diluted in deionized water by centrifuging until the pH was 7. The obtained sample was dried in a vacuum oven at 80 ℃ for 24 h.

Characterisation of CNTs

The carbon yield of each catalytic reaction was defined based on catalytic performance and was calculated as shown in Eq. (1) according to ref. (Zhuo and Levendis 2014; Modekwe et al. 2020):

$$Yield\,(\%) = \frac{mass\ of\ deposit\ -\ mass\ of\ catalyst}{mass\ of\ catalyst} \times 100\% \tag{1}$$

The microstructure of purified nanotubes was obtained using JEM-2100 transmission electron microscopy (TEM) (JEOL, Japan) operated at 200 kV.

The quality of purified nanomaterials was ascertained using the Raman spectroscopy technique with WITec focus innovations Raman Spectrometer (WITec, Germany). Spectra were collected at an excitation laser wavelength of 532 nm in the Raman shift frequency of 1000–3500 cm^{-1}.

Modelling

Artificial neural network (ANN) is an efficient tool for detecting the patterns in different variables within a dataset such that the pattern could be utilized in training, testing, and modelling similar datasets (Çolak et al. 2021). ANN learns and takes a broad view from cases and practice (Aci and Avci 2016). Recently, the rise in the use of ANN for prediction is owing to its strength in handling various datasets including nonlinear and complex data (Sedighi et al. 2011; Kusumo et al. 2019). There are several neural networks that ANN utilizes, they include Cascade-Forward Neural Network (CFNN), Feed-Forward Neural Network (FFNN), Generalized Regression Neural Network (GRNN), and Function Fitting Neural Network (FITNET) (Aci and Avci 2016). In this work, FITNET was utilized to identify the connecting pattern in the experimental datasets, and utilized to train and develop a model that can be used to predict the quality and yield of CNTs produced from waste polypropylene plastics, and this is because of its potential to properly fit the relationship between inputs and response variables (Aci and Avci 2016). The framework of a FITNET tool is identified in Fig. 1. Matlab software with an inbuilt toolbox for machine learning prediction using ANN was utilized as the software for the predictive model generation. The predictors that were supplied as input parameters to the FITNET, together with the responses are shown in Fig. 2. In essence, there were four inputs and two responses.

Training, validation, and testing (TVT)

When using neural networks for developing a predictive model, one of the main tasks is avoiding overfitting, to achieve this, it is important to divide datasets into training, validation, and testing sets. The training set helps to evaluate the parameters of the model, the validation set assists in establishing the potential of the model to generalize,
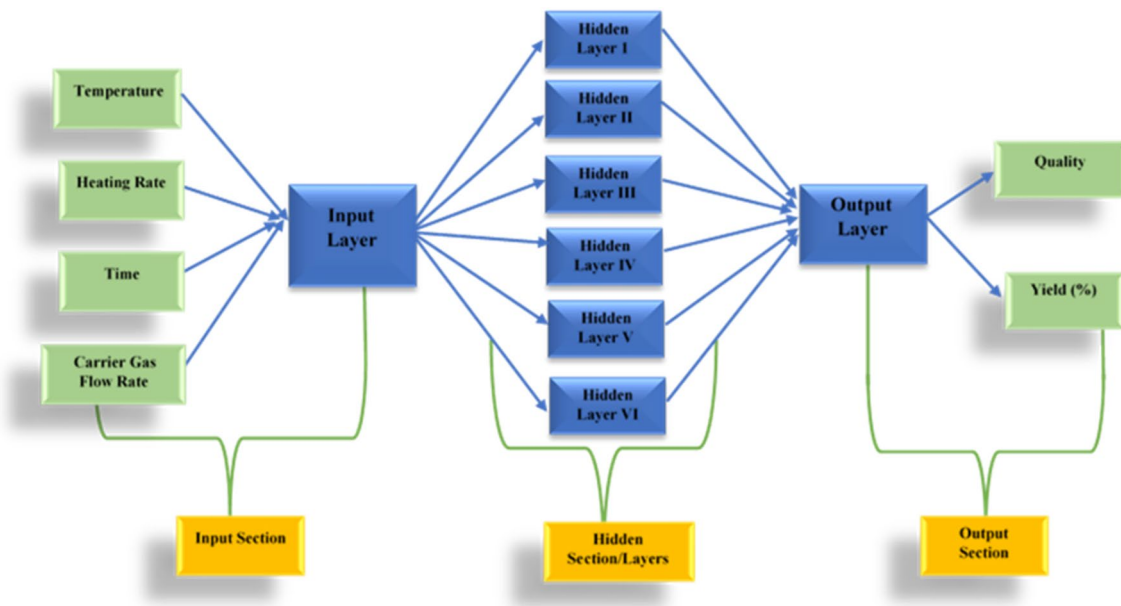
Fig. 1 Framework of a FITNET

Function Fitting Neural Network
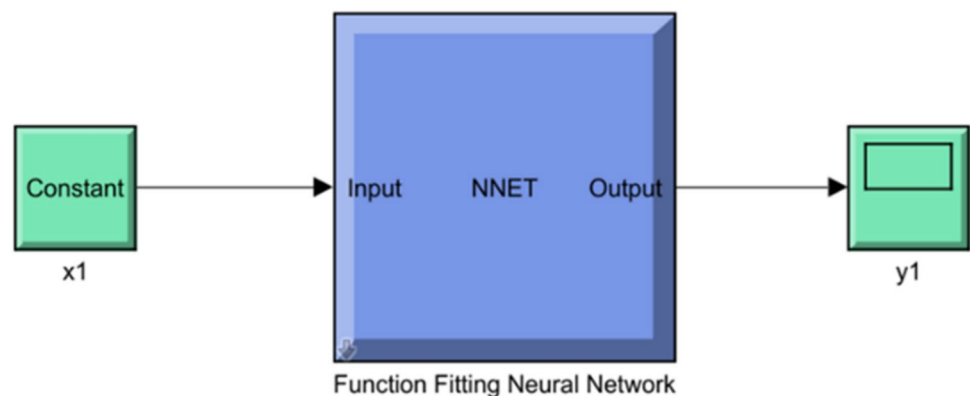
Fig. 2 Pictorial representation of the input, hidden, and output layers of a neural network
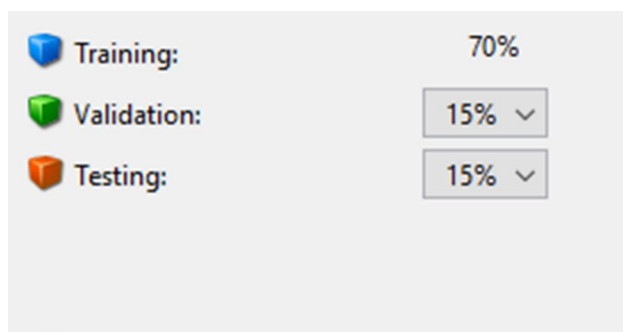

Fig. 3 Rationing of datasets for TVT

and the test set helps in monitoring the performance of the developed model (Sedighi et al. 2011). Furthermore, in the training, validating, and testing of datasets using ANN, there are different algorithms that can be utilized, they include Bayesian Regularization, Scaled Conjugate Gradient, and Levenberg–Marquardt (Baghirli 2015; Parmar et al. 2017; Bharati et al. 2021). In this paper, the Levenberg–Marquardt algorithm was employed; this is because of its ability to train datasets with small and medium size; besides, it is quick with steady convergence (Yu and Wilamowski 2011). In rationing the available datasets, 70% of the datasets were utilized for training, 15% for validation, and 15% for testing (Fig. 3). Besides, three hidden neurons (5,8, and 10) were utilized (Fig. 4).

Model performance indicator (MPI)

Generally, the MPI for a FITNET model of ANN is measured using mainly MSE and R. MSE is regarded as the mean square error, it estimates the difference between the actual response's mean square and that of the predicted response (Lavrakas 2013). R stands for correlation coefficient and estimates the correlation between the actual and predicted response (Aci and Avci 2016). Importantly, the higher the values of R, the better the model, and the closer the predicted response is to the actual, in contrast, the lower the MSE, the better the model. Mathematically, MSE and R values are expressed using Eqs. 2 and 3, respectively.

$$R = \sqrt{1 - \left(\frac{\sum_{J=1}^{N} \left(Y_j - Y_p \right)^2}{\sum_{J=1}^{N} \left(Y_j - Y_m \right)^2} \right)} \qquad (2)$$

$$MSE = \frac{1}{N} \sum_{J=1}^{N} \left(Y_j - Y_p \right)^2 \qquad (3)$$

$MSE = Mean\, Square\, Error$

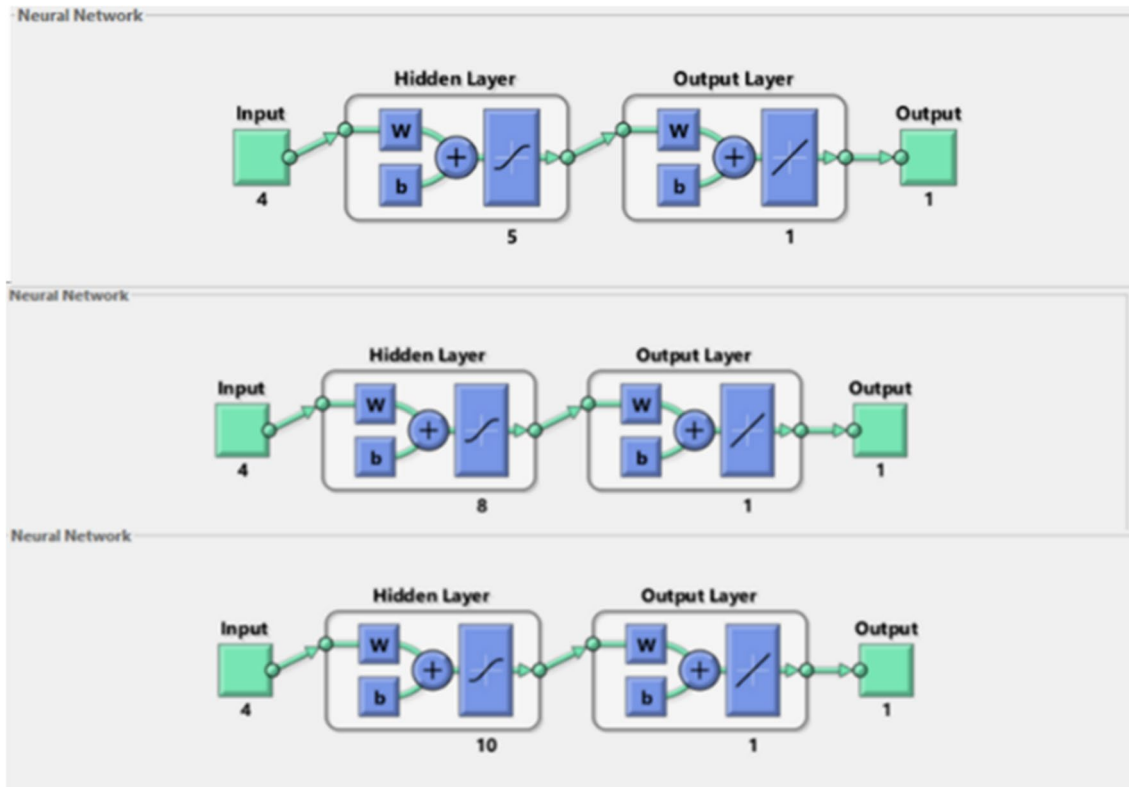$N = Number\, of\, data\, points\, used\, in\, testing$

$Y_j = actual\, response$

Fig. 4 FITNET model with 5,8, and 10 hidden neurons

Y_p = *predicted response*

Y_m = *mean value of the actual response*

Results and discussion

The experimental parameters and their corresponding responses in terms of obtained quality and yield of as-produced plastic-derived CNTs for all runs are presented in Table 2. Likewise, the experimental and predicted values with the overall MSEs of responses for the quality and yield of CNTs are presented in Table 2.

Response 1 is a measure of CNT quality expressed in terms of the Intensity ratio of G/D obtained from Raman Spectroscopy analysis. Response 2 expressed the yield of synthesized CNTs obtained according to Eq. 1.

Characterization of CNTs

TEM images of some selected runs based on maximum and minimum CNTs yield as well as quality were shown in Fig. 5. TEM micrograph images confirmed the presence of hollow core filamentous carbons confirmed to be multi-walled carbon nanotubes (MWCNTs). The average diameter distribution of all as-synthesized CNTs was around 20–50 nm and up to a few microns in length. Several encapsulated metal catalysts could be seen attached to the tips of the nanotubes indicating a tip-growth model. Figure 5B, E, and F showed distorted, uneven nanotubes walls, however, no visible amorphous carbons could be observed.

The yield of synthesized carbon (MWCNTs) was obtained using Eq. (1). As can be observed in Table 2, maximum and minimum yields were obtained with runs 9 and 7, respectively.

Raman spectroscopy analysis was carried out to check for the structure of amorphous and/or graphitic carbon and evaluate the purity of CNTs. Raman spectra of CNTs of some selected runs are presented in Fig. 6 at a wavelength of 1000–3500 cm^{-1}. These selected runs are runs that presented optimal and minimal CNTs yield and quality. The Raman spectra are dominated by three characteristic vibration bands of the Raman vibrations of carbonaceous materials: the D-band at ~ 1344 cm^{-1} emanated from amorphous carbon or structural disordered carbon within graphene structure; the G-band at ~ 1572 cm^{-1} from the sp^2 stretching vibration of graphitic structures and characteristics of

Table 2 Experimental process variable data with corresponding experimental, predicted, and overall error values of responses in terms of CNTs yield and CNTs quality

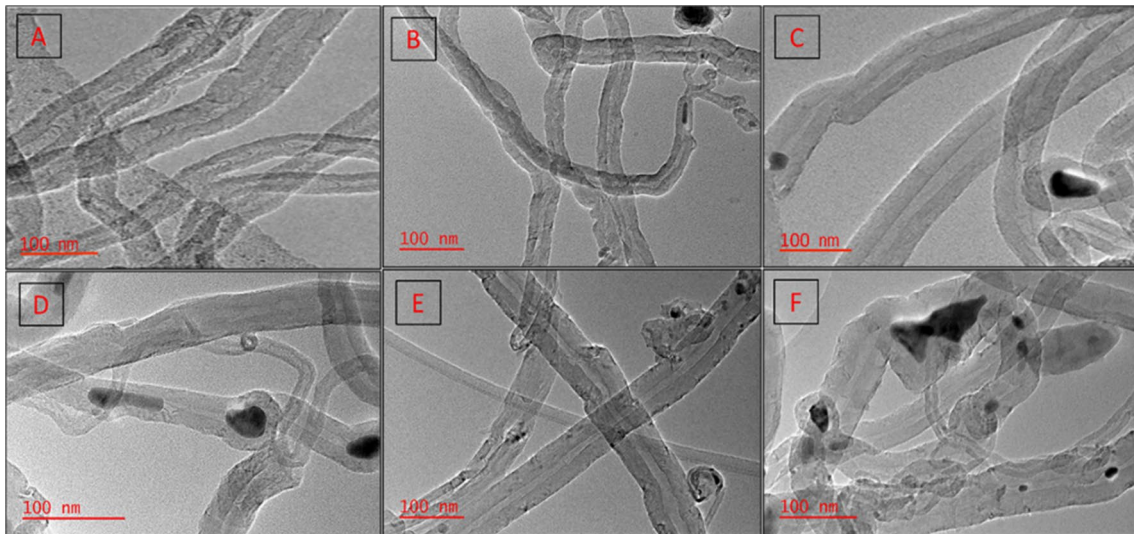| Numerical factors	Factor 1	Factor 2	Factor 3	Factor 4	Response 1 (experimental quality)	Predicted quality	Overall error	Response 2 (experimental yield)	Predicted yield	Overall error
Run	A: Synthesis temperature (°C)	B: Heating rate (°C/min)	C: Time (min)	D: N_2 Flow rate (mL/min)	Quality (I_G/I_D)	Quality (I_G/I_D)	Quality (I_G/I_D)	Yield (%)	Yield (%)	Yield (%)
1	600	5	25	120	1.02	1.1011	−0.0812	65.5	62.0194	3.4806
2	600	10	30	120	0.93	0.9682	−0.0382	58.7	58.5375	0.1625
3	700	10	25	70	1.00	1.0019	−0.0020	59.3	64.8481	−5.5481
4	800	15	25	100	1.46	1.2662	0.1938	39.2	52.2480	−13.0481
5	800	5	25	100	1.60	1.6028	−0.0029	57.7	63.3444	−5.6444
6	800	10	30	100	1.30	1.3038	−0.0038	45.0	47.3447	−2.3447
7	600	10	20	100	1.00	1.0836	−0.0036	32.0	31.6117	0.3883
8	800	10	20	70	1.16	1.1637	−0.0037	45.0	48.7494	−3.7494
9	600	15	25	120	0.98	0.9962	−0.0162	64.5	55.4469	9.0531
10	700	15	30	120	1.17	1.1847	−0.0147	57.1	60.1361	−3.0361
11	700	5	30	100	1.09	1.1015	−0.0115	54.5	54.5238	−0.0238
12	700	5	20	100	1.12	1.1261	−0.0061	34.5	42.3037	−7.8037
13	700	15	20	120	1.09	1.1008	−0.0109	58.3	58.1375	0.1625

Fig. 5 TEM micrographs of purified CNTs synthesized over NiMo/CaTiO₃ catalyst at different process parameters, Images (**A–F**) denote run number 1, 2, 4, 5, 7, and 9, respectively

Fig. 6 Raman spectra of purified CNTs over NiMo/CaTiO₃ catalyst under various process conditions, **a–f** indicates run number 7, 2, 1, 9, 5 and 4, respectively
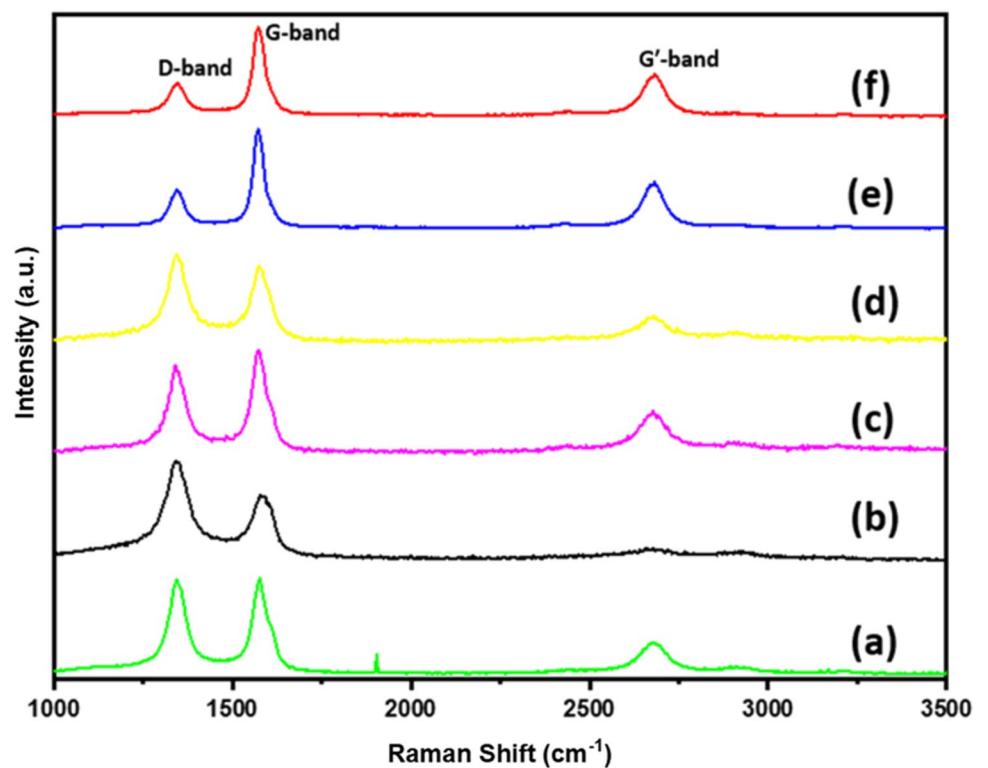
graphitic carbon; and the G′ at ~ 2682 cm^{-1} arises from the second-order elastic scattering process of two phonons, indicating the purity of carbons (Dresselhaus et al. 2005). It could be observed that in Fig. 6b there is a shift in the G-band at ~ 1580 cm^{-1} and a very diminished peak for G′-band was also observed signifying increased defective and disordered graphite structure (Modekwe et al. 2021c).

The intensity (I_G/I_D) ratio, depicts the relative intensity of the G- and D-bands of a Raman spectrum, which is an indicator of the degree of graphitization and quality of CNTs. Figure 6e, f for runs 5 and 4 presented the highest I_G/I_D value showing improved structural integrity in their graphene walls compared to others as shown in Table 2 (Response

1). Figure 6b showed the least graphitized and quality CNT which agrees with the result obtained in TEM.

Model result

A total of 42 runs of TVT of the datasets were performed for the quality and yield responses. This resulted in the generation of various MSE (126 total data values), and R (168 data values), The R values include that of the training, validation, testing, and the overall value. For the purpose of generalization, the value of the overall R was used to determine the performance of the system before the MSE was considered. Based on this, the TVT run with the highest overall R value was chosen as the best model for the prediction of the quality and yield of CNTs. with any of the runs being the possibly preferred predictive model. However, the preferred model was explicitly chosen based on the overall R value of each run, with a non-negative value of R in any of the training, validation, and testing value.

For the quality of the CNT, the best overall R value is 0.94753 which could mean about 95% model performance,

while that of the yield is 0.87445: about 87% performance (Fig. 7). The MSE (mean square error) and overall R (correlation coefficient) value of the entire 42 runs are presented in Table 3 and Table 4.

For the quality of the CNTs, the error histogram, and validation performance is presented in Fig. 7, with the best validation performance at an epoch value of 2. This implies that the frequency of passes of the whole dataset used for TVT before the best overall R value was obtained for that specific iteration was completed at an epoch value of 2. Besides, in the validation performance, there was no overfitting; meaning that the TVT task learned from the raw data and did not memorise them (Gandhi 2018). Furthermore, the best validation performance of 0.022079 shown in Fig. 8 translates to the validation MSE value for the choicest model for predicting quality (21st run in Table 3). For the yield, the best validation performance was 40.9797, obtained at an epoch value of 1 (Fig. 9), and translates to the validation MSE value for the choicest model for predicting yield (19th run in Table 4). The error histogram (Fig. 9) presents the error obtained from the difference between the actual and
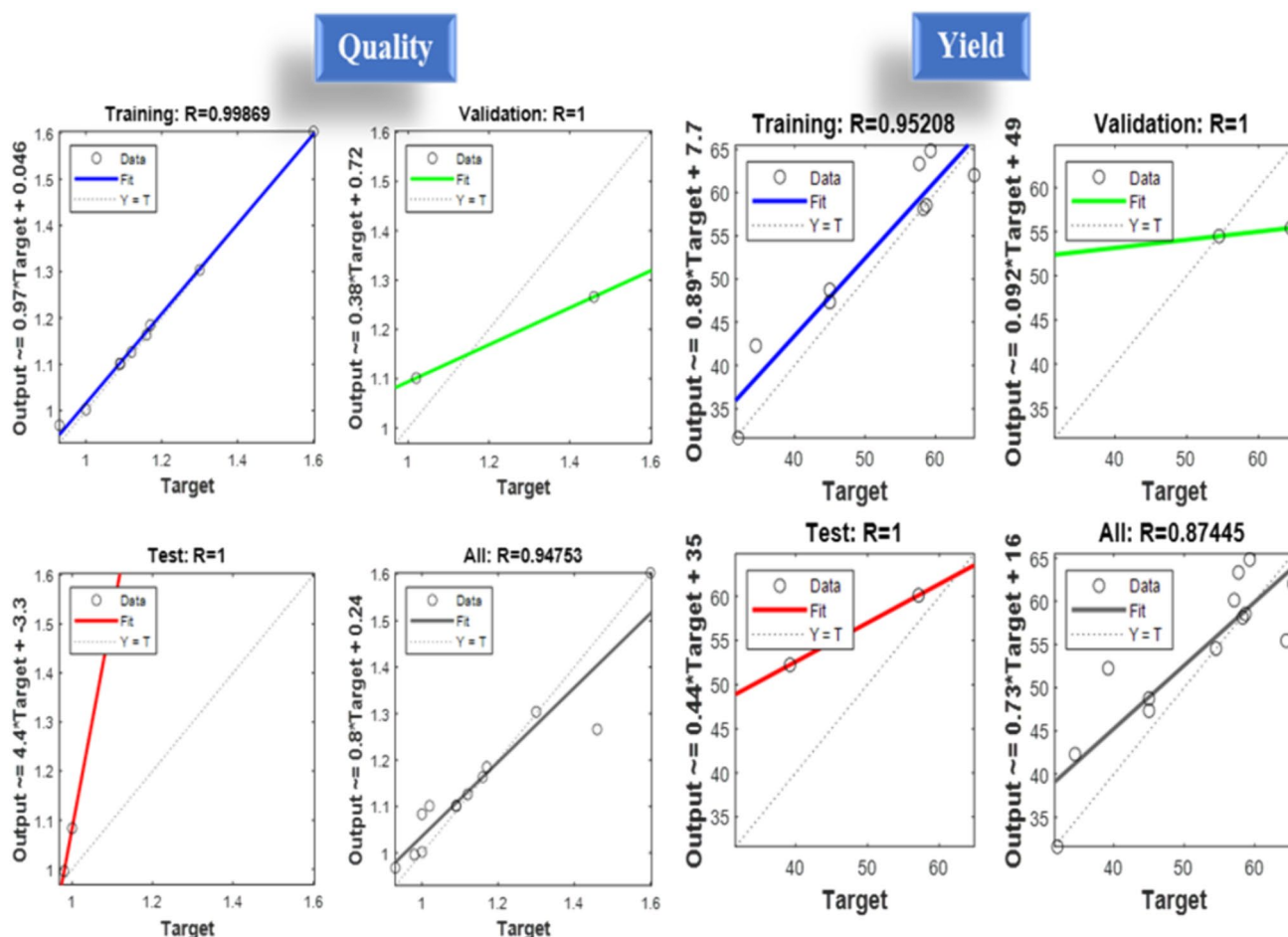

Fig. 7 Neural network models with training, validation, testing, and all prediction set

Table 3 The CNTs quality MSE and overall R value of the entire 42 runs

Quality			
runs	Training MSE	Validation MSE	Testing MSE	Overall R value
1	5.35E-16	8.46E-02	1.17E-02	8.00E-01
2	9.42E-03	8.07E-02	4.91E-02	5.35E-01
3	1.11E-03	1.00E-02	7.27E-02	8.13E-01
4	1.49E-09	3.80E-02	9.82E-02	8.10E-01
5	4.92E-01	2.99E-02	5.44E-01	-3.74E-01
6	1.51E-02	1.68E-02	1.46E-02	8.37E-01
7	1.32E-02	4.97E-03	2.55E-01	4.67E-01
8	8.13E-17	2.29E-02	1.14E-01	6.68E-01
9	2.51E-06	1.72E-02	5.09E-02	8.93E-01
10	1.86E-02	2.33E-03	5.91E-02	7.66E-01
11	2.72E-04	1.18E-01	1.49E-02	7.15E-01
12	4.74E-03	5.63E-03	5.21E-02	8.98E-01
13	1.72E-03	1.01E-01	3.95E-04	7.80E-01
14	3.09E-01	4.72E-02	4.67E-01	-5.65E-01
15	5.05E-17	1.26E-02	3.06E-02	9.07E-01
16	1.08E-01	2.36E-02	3.01E-01	4.80E-01
17	1.18E-04	6.07E-02	2.11E-02	8.51E-01
18	3.37E-17	2.25E-02	4.00E-01	6.25E-01
19	1.00E-02	1.21E-03	1.18E-02	9.14E-01
20	1.43E-02	8.83E-03	5.91E-02	7.22E-01
21	**2.23E-04**	**2.21E-02**	**3.63E-03**	**9.48E-01**

Table 4 The CNTs yield MSE and overall R value of the entire 42 runs

Yield			
Runs	Training MSE	Validation MSE	Testing MSE	Overall R
1	3.57E+02	6.02E+01	5.29E+02	−1.50E-01
2	1.49E+02	1.01E+02	4.91E+02	−1.86E-02
3	2.96E+02	1.84E+01	2.65E+02	7.54E-02
4	2.47E+01	6.41E+01	2.90E+02	6.90E-01
5	8.55E+01	6.23E+02	4.30E+02	−3.79E-02
6	1.67E+02	1.52E+01	2.06E+02	3.14E-01
7	1.20E+02	1.17E+01	1.39E+02	4.65E-01
8	6.46E+01	7.06E+01	4.22E+02	4.26E-01
9	2.32E+01	7.01E+01	4.98E+01	8.71E-01
10	1.84E+01	3.98E+01	2.15E+02	8.03E-01
11	1.66E-04	5.27E+01	4.03E+02	6.72E-01
12	1.37E+00	1.72E+01	7.09E+02	6.29E-01
13	1.80E+01	2.11E+02	2.95E+02	5.28E-01
14	2.90E+01	1.96E+01	5.12E+02	5.90E-01
15	2.53E+01	2.40E+02	2.61E+02	6.97E-01
16	9.54E+01	1.86E+01	2.46E+01	7.71E-01
17	7.02E+00	2.96E+02	6.48E+02	4.36E-01
18	1.19E+03	7.76E+01	5.55E+02	−2.08E-01
19	**1.73E+01**	**4.10E+01**	**8.97E+01**	**8.74E-01**
20	1.25E+01	3.60E+02	5.20E+02	4.59E-01
21	2.27E-01	2.48E+02	1.68E+02	7.56E-01

predicted response during the TVT after the dataset was trained in a forward manner, while the bins represent the number of error values on the error histogram.

For the quality of CNTs, the error obtained during the training, testing, and validation varied from −0.07665 to 0.1889 (Fig. 8), the small variation further confirms that the margin for error during the predictive model generation is small, and confirms the ability of ANN to be utilized in developing a predictive model for CNT's quality. For the yield of CNT, the error ranged from −12.5 to 8.501 (Fig. 9), this is a bit high and is reflected in the R-value of 0.87445, however, this does not discredit the potential of ANN in developing a model for the prediction of CNTs yield, perhaps, could imply that for future research there should be a more raw dataset that ought to be utilized for developing a predictive model for the yield of CNT, since the performance of a predictive model is most times strengthened by the number of data (De Fortuny et al. 2013; Ray 2015; Gandhi 2018). Nonetheless, the model would also assist in giving an estimate of what the yield of CNTs produced under the same condition and the number of runs would produce. Therefore, the MSE values of the best predictive model on the quality and yield of CNTs were obtained at the 21st and 19th run respectively as presented in Table 3 and Table 4.

After the TVT, and choosing the best R value, a predictive model was developed that can be used on a similar dataset with the same predictive parameters. In simple terms, the predictive model is presented in Eqs. 4, 5, 6, 7, and 8.

$$y_1 = netX_1 \tag{4}$$

$$y_2 = netX_2 \tag{5}$$

$$[X_1, X_2] = [X_{synthesistemp} X_{heatingrate} X_{time} X_{carriergasflowrate}] \tag{6}$$

$$y_{quality} = net[X_{synthesistemp} X_{heatingrate} X_{time} X_{carriergasflowrate}] \tag{7}$$

$$y_{yield} = net[X_{synthesistemp} X_{heatingrate} X_{time} X_{carriergasflowrate}] \tag{8}$$

where, y_1 and y_2 represents the possible values of the quality and yield respectively, based on a set of X_1 and X_2 respectively. It is important that X_1 and X_2 represents a matrix of a set of input parameters for determining the quality and yield of CNTs. net stands for the neural network model that would be called using the code generated from data TVT to estimate the possible values of y (quality and yield) once the input parameters (Xs) are supplied. The code is provided in the Online Resource.
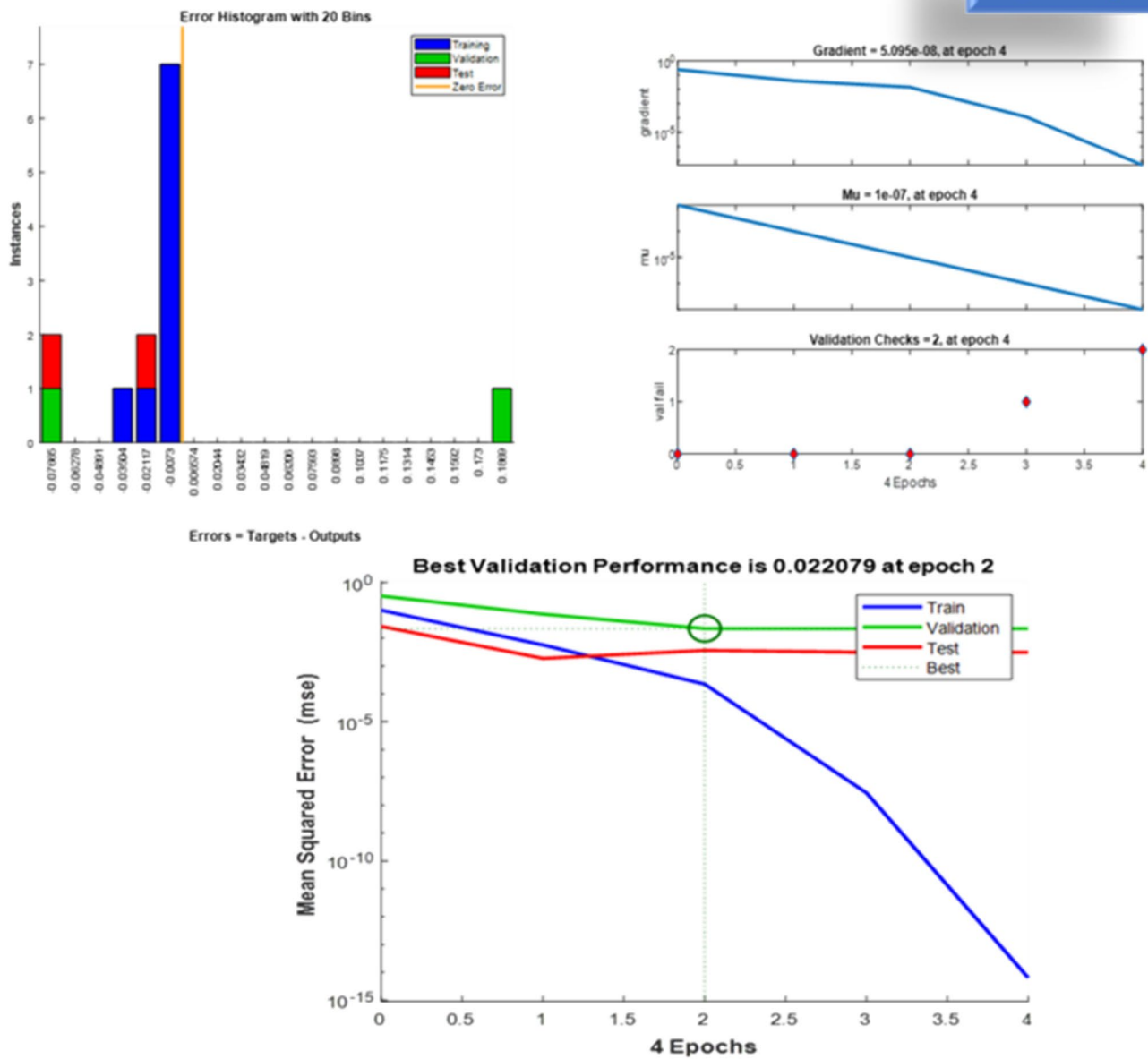
Fig. 8 CNTs quality error histogram, and validation performance

Conclusion

To the best of our knowledge, we reported for the first time a successful predictive model for the performance characteristics (yield and quality) of waste polypropylene derived-MWCNTs synthesized over NiMo/CaTiO$_3$ catalyst in a single-stage CVD reactor using artificial neural network (ANN). Here, the predicted model showed an acceptable agreement between experimental datasets of CVD growth input parameters (synthesis temperature, furnace heating rate, residence time, and inert gas flow rate) and the performance features (yield and quality; I$_G$/I$_D$) of obtained MWCNTs, with the coefficient of correlation of 0.94753 and 0.87445 for the predicted CNTs quality and yield, respectively. Furthermore, the validation MSE for the quality and yield of CNTs are 0.022079 and 40.9797 respectively. The error range for yield was a bit high, nevertheless, it does not discredit the potential of
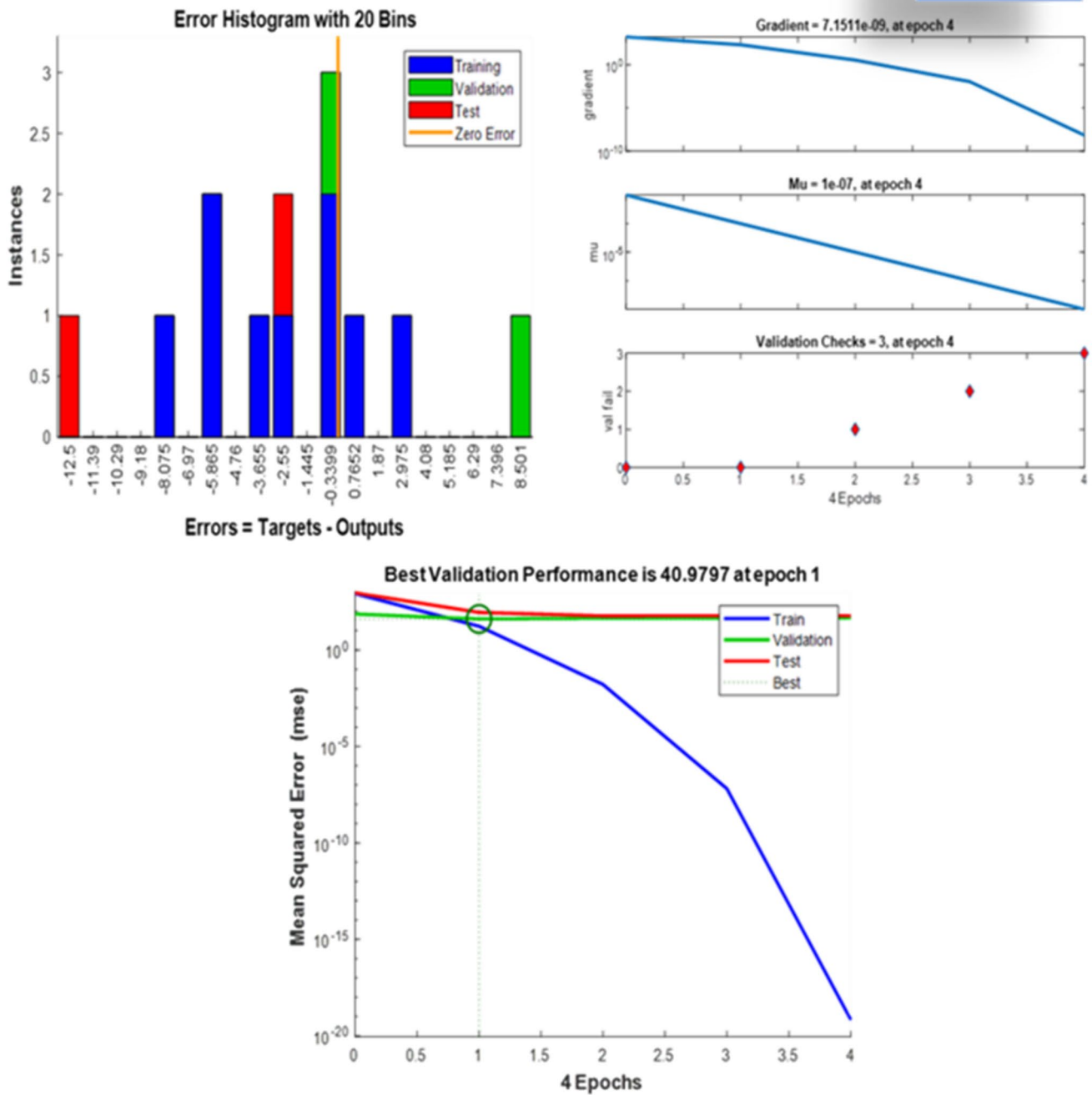
Fig. 9 CNTs yield error histogram, and validation performance

ANN in developing a model for the prediction of CNTs yield. However, the model accuracy can be enhanced by increasing the experimental raw dataset since the trained ANN is restricted by a small set of experimental datasets.

Hence, the results obtained justifies further studies in this area.

Declarations

References

Abad SNK, Ganjeh E, Zolriasatein A et al (2017) Predicting carbon nanotube diameter using artificial neural network along with characterization and field emission measurement. Iran J Sci Technol Trans A Sci 41:151–163. https://doi.org/10.1007/s40995-017-0198-9

Aci M, Avci M (2016) Artificial neural network approach for atomic coordinate prediction of carbon nanotubes. Appl Phys A Mater Sci Process 122:1–14. https://doi.org/10.1007/s00339-016-0153-1

Baghirli O (2015) Comparison of Lavenberg–Marquardt, scaled conjugate gradient and Bayesian regularization backpropagation algorithms for multistep ahead wind speed forecasting using multilayer perception feedforward neural network

Bajad G, Vijayakumar RP, Rakhunde P et al (2017) Processsing of mixed-plastic waste to fuel oil, carbon nanotubes and hydrogen using multi-core reactor. Chem Eng Process Process Intensif 121:205–214. https://doi.org/10.1016/j.cep.2017.09.011

Bazargan A, Mckay G (2012) A review - Synthesis of carbon nanotubes from plastic wastes. Chem Eng J 195–196:377–391. https://doi.org/10.1016/j.cej.2012.03.077

Bharati S, Rahman MA, Podder P et al (2021) Comparative performance analysis of neural network base training algorithm and neuro-fuzzy system with SOM for the purpose of prediction of the features of superconductors. Adv Intell Syst Comput 1181:69–79. https://doi.org/10.1007/978-3-030-49342-4_7

Çolak AB, Güzel T, Yıldız O, Özer M (2021) An experimental study on determination of the shottky diode current-voltage characteristic depending on temperature with artificial neural network. Phys B Condens Matter 608:412852–412852. https://doi.org/10.1016/j.physb.2021.412852

Das R, Hamid SBA, Ali ME et al (2015) Carbon nanotubes characterization by X-ray powder diffraction–a review. Curr Nanosci 11:1–13. https://doi.org/10.2174/1573413710666140818210043

De Fortuny EJ, Martens D, Provost F (2013) Predictive modeling with big data: is bigger really better? Big Data 1:215–226. https://doi.org/10.1089/big.2013.0037

Deniz CU, Yasar M, Klein MT (2017) Stochastic reconstruction of complex heavy oil molecules using an artificial neural network. Energy Fuels 31:11932–11938. https://doi.org/10.1021/acs.energyfuels.7b02311

Dresselhaus MS, Dresselhaus G, Saito R, Jorio A (2005) Raman spectroscopy of carbon nanotubes. Phys Rep 409:47–99. https://doi.org/10.1016/j.physrep.2004.10.006

Gandhi R (2018) Improving the performance of a neural network. Towar. Data Sci. https://towardsdatascience.com/how-to-increase-the-accuracy-of-a-neural-network-9f5d1c6f407d. Accessed 3 Jul 2021

Krasnikov DV, Khabushev EM, Gaev A et al (2023) Machine learning methods for aerosol synthesis of single-walled carbon nanotubes. Carbon 202:76–82. https://doi.org/10.1016/j.carbon.2022.10.044

Kukovecz A, Mehn D, Nemes-Nagy E et al (2005) Optimization of CCVD synthesis conditions for single-wall carbon nanotubes by statistical design of experiments (DoE). Carbon 43:2842–2849. https://doi.org/10.1016/j.carbon.2005.06.001

Kusumo F, Mahlia TMI, Shamsuddi AH et al (2019) The effect of multi-walled carbon nanotubes-additive in physicochemical property of rice brand methyl ester: optimization analysis. Energies 12:3291. https://doi.org/10.3390/en12173291

Lakovlev VY, Krasnikov DV, Khabushev EM et al (2019) Artificial neural network for predictive synthesis of single-walled carbon nanotubes by aerosol CVD method. Carbon 153:100–103. https://doi.org/10.1016/j.carbon.2019.07.013

Lavrakas P (2013) Mean Square Error (MSE). In: Encyclopedia of Survey Research Methods. Sage Publications, Inc.

Lefrant S, Baibarac M, Baltog I (2009) Raman and FTIR spectroscopy as valuable tools for the characterization of polymer and carbon nanotube based composites. J Mater Chem 19:5690–5704. https://doi.org/10.1039/b821136a

Lehman JH, Terrones M, Mansfield E et al (2011) Evaluating the characteristics of multiwall carbon nanotubes. Carbon 49:2581–2602. https://doi.org/10.1016/j.carbon.2011.03.028

Modekwe HU, Mamo MA, Daramola MO, Moothi K (2020) Catalytic performance of calcium titanate for catalytic decomposition of waste polypropylene to carbon nanotubes in a single-stage CVD reactor. Catalysts 10:1030. https://doi.org/10.3390/catal10091030

Modekwe HU, Mamo M, Moothi K, Daramola MO (2021a) Polypropylene waste-derived carbon nanotubes (CNTs) via single-stage CVD technique: determination of crystallinity. IOP Conf Ser Mater Sci Eng 1107:012067. https://doi.org/10.1088/1757-899x/1107/1/012067

Modekwe HU, Mamo M, Moothi K, Daramola MO (2021b) Synthesis of bimetallic NiMo/MgO catalyst for catalytic conversion of

waste plastics (polypropylene) to carbon nanotubes (CNTs) via chemical vapour deposition method. Mater Today Proc 38:549–552. https://doi.org/10.1016/j.matpr.2020.02.398

Modekwe HU, Mamo MA, Moothi K, Daramola MO (2021) Effect of different catalyst supports on the quality, yield and morphology of carbon nanotubes produced from waste polypropylene plastics. Catalysts 11(6):692. https://doi.org/10.3390/catal11060692

Modekwe HU, Daramola MO, Mamo MA, Moothi K (2024) Recent advancements in the use of plastics as a carbon source for carbon nanotubes synthesis-a review. Heliyon 10:e24679. https://doi.org/10.1016/j.heliyon.2024.e24679

Parmar R, Shah M, Shah MG (2017) A comparative study on different ANN techniques in wind speed forecasting for generation of electricity. IOSR J Electr Electron Eng 12:19–26. https://doi.org/10.9790/1676-1201031926

Raji K, Sobhan CB (2013) Simulation and modeling of carbon nanotube synthesis: current trends and investigations. Nanotechnol Rev 2:73–105. https://doi.org/10.1515/ntrev-2012-0038

Rao R, Pint CL, Islam AE et al (2018) Carbon nanotubes and related nanomaterials: critical advances and challenges for synthesis toward mainstream commercial applications. ACS Nano 12:11756–11784. https://doi.org/10.1021/acsnano.8b06511

Ray S (2015) How to increase accuracy of machine learning model. https://www.analyticsvidhya.com/blog/2015/12/improve-machine-learning-results/. Accessed 3 Jul 2021

Sedighi M, Keyvanloo K, Towfighi J (2011) Modeling of thermal cracking of heavy liquid hydrocarbon: application of kinetic modeling, artificial neural network, and neuro-fuzzy models. Ind Eng Chem Res 50:1536–1547. https://doi.org/10.1021/ie1015552

Yang Y, Lim S, Wang C et al (2004) Statistical analysis of synthesis of Co-MCM-41 catalysts for production of aligned single walled carbon nanotubes (SWNT). Microporous Mesoporous Mater 74:133–141. https://doi.org/10.1016/j.micromeso.2004.06.012

Yu H, Wilamowski BM (2011) Levenberg–Marquardt training. In: Irwin J (ed) Intelligent Systems, 2nd edn. CRC Press, Boca Raton, pp 1–16

Zhuo C, Levendis YA (2014) Upcycling waste plastics into carbon nanomaterials: a review. J Appl Polym Sci 131:1–14. https://doi.org/10.1002/app.39931